IFSCC 2025 full paper (1168)

In vitro tear film instability: A new physico-chemical approach to evaluate eye discomfort

Swati Kaushik[1*], Laurent Guillet-Revol[1], Florian Dano[1], Thanh Pham Kim Nguyet[1], Koji Endo[2], Masanori Orita[2], Ingrid Gamba[1], Yoshimune Nonomura[3] and Noémie de Crozé[1]

[1]L'Oréal Research & Innovation, France; [2]L'Oréal Research & Innovation, Japan; [3] Yamagata University Faculty of Engineering, Japan

1. Introduction

Ocular tolerance assessment presents a significant challenge for the cosmetics industry [1], particularly for shampoos formulated for children and babies, a population with increased risk of ocular exposure to these products. While ocular irritation which is largely a damage to cornea (and surrounding tissues) is a well-researched area medically speaking [2,3,4], ocular discomfort, characterized by sensations such as dry eye, tingling, lack of clarity in vision and prickling, remains poorly understood. A possible reason is because eye discomfort encountered during the interaction between the eye and a cosmetic formula, is a subjective sensation without involving damage to tissue, making it difficult to evaluate. An understanding of human tear film (TF) physiology is crucial for elucidating the mechanisms underlying ocular discomfort caused by cosmetic formulas. The tear film (TF) protects the cornea from possible external aggressions such as dust, particles etc [5]. It consists of three distinct layers named (from the deepest to the outermost) (Figure 1), the mucin (I), the aqueous layer (II) and the lipid layer (III).

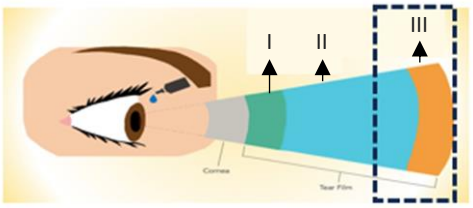

Figure 1 Schematic representation of the human tear film

Directly in contact with the cornea, there is a thin film of mucin proteins present in large proportions in the mucus. Then comes the aqueous layer of the human tear film, it is mainly made up of water and contains many biochemical entities such as electrolytes, proteins and their metabolites [6,14]. The most abundant protein in the aqueous phase is the Lipocalin [18]. It's an amphiphilic protein that potentially plays a major role in the spreading of the tear film over the cornea and in the interactions between the aqueous phases and neighboring phases. The total thickness of these first two layers is generally between 6-10 µm in a healthy human eye [6,10]. Finally, the outermost layer is a lipid layer which is the thinnest of the 3 layers and is

composed mainly of lipids. It is the meibomian glands that secrete the lipid layer of the tear film, which plays a key role in reducing evaporation of the underlying aqueous layer [18]. Several scientific studies have linked lipid layer deficiency to dry eye disease [7,8]. The normal blinking mechanism [9] (10-12 blinks per minute, with an approximate 5 s interval between each blink) replenishes the lipid layer, and distributes it across the aqueous layer like a curtain [5,18]. Many times physiological changes compromise the lipid layer integrity leading to an increased aqueous evaporation and subsequent dry eye disease [12,13], a condition affecting approximately 30% of the global population [12]. Given the established connection between dry eye, lipid layer deficiency, and ocular discomfort, we hypothesize that cosmetic product exposure with its associated ingredients such as surfactants, preservatives, and solvents, disrupts the lipid layer, causing it to break up into smaller lenses [13,16]. This disruption of lipid layer integrity could possibly be a potential causative factor in the sensation of ocular discomfort. This study introduces a novel in vitro approach to assess the discomfort potential of formulations by investigating the interplay between a model tear film and formulas. Here, we investigate the spreading dynamics and stability of a model tear film. We analyze the spreading characteristics of microliter-sized droplets of lipid phase of the tear film deposited onto an aqueous substrate composed of a 1:1 mixture of aqueous phase of tear film and shampoo. A controlled experimental setup was designed to observe droplet spreading at a constant temperature. The spreading dynamics were quantitatively assessed using Tanner's law [15]. Furthermore, the stability of the lipid phase was evaluated by measuring the breakup time (BUT) of the spreading film. This physico-chemical approach provides a valuable pre-clinical tool for screening formulations, aiming to optimize clinical trials by improving in vitro predictions of ocular discomfort.

2. Materials and Methods

2.1 Model Lacrymal film

In order to study a system close to the real human tear film, we reconstituted model phases of the aqueous and lipid layers similar to the layers of tear film according to the recipe by Rondot *et al* [17]. The aqueous and the lipid phase contain ingredients that are structurally, behaviourly and proportionally similar to the ones actually found in the tear film (see Table I).

Table I Composition of the aqueous and lipid model phases.

Phase	Ingredient	Mass Proportion (%)
Aqueous phase	Deionized water	98,36
	Potassium Bicarbonate	0,8
	Bovine serum albumin	0,5
	Sodium bicarbonate	0,18
	Sodium chloride	0,65
	Glucose	0,65
	Urea	0,03
Lipid phase	Cholesterol Oleate	40
	Myristyle Myristate	40
	L-α-phosphatidylcholine	15
	Cottonseed oil	5

2.2 Clinical evaluation

Clinical assessment of the shampoos were established by ophthalmologists after monitoring the ocular prickling and redness of conjonctiva in standardized conditions on 15 volunteers. The shampoos were then classified as good and poor clinical profile based on the average scores.

2.3 Experimental study of spreading dynamics

The spreading experiment consists of depositing a 5 µL drop of the lipid phase in a petri dish containing the aqueous substrate (1:1 mixture of the aqueous phase and a 1% dilution of the shampoo in milliQ water). We used 1% diluted shampoo to simulate the diluted concentration expected upon exposure to eye during hair rinsing. We then observed the lipid droplet spread over the aqueous substrate. The droplet were assumed to spread circularly. The evolution of radius, r, of the lipid droplet as a function of time, t, was adjusted with Tanner's law ($r(t) = k.t^n$) which governs the spreading dynamics of non volatile Newtonian liquids [15].

2.3.1 Experimental setup

The entire setup was placed inside an oven maintained at a constant temperature (as shown in Figure 2), a glass petri dish is placed on a black painted metal support in order to avoid unnecessary reflections. A white light plate was used to illuminate the petri dish. The black background of the petri dish holder, and the light made it possible to properly distinguish the aqueous and lipid phases, which were colourless and difficult to discern without suitable lighting. A smartphone camera (lens, Sony IMX800) was used to capture the evolution of the droplet after it was deposited over the aqueous substrate at recording speed of 60 fps (frames per second). While the tubing was always outside the oven, the glass capillary was kept inside the oven. The capillary was previously treated by commercially available solution to form an oleophobic coating on the surface. This system was set up to generate droplets of 5 µL of the model lipid phase.

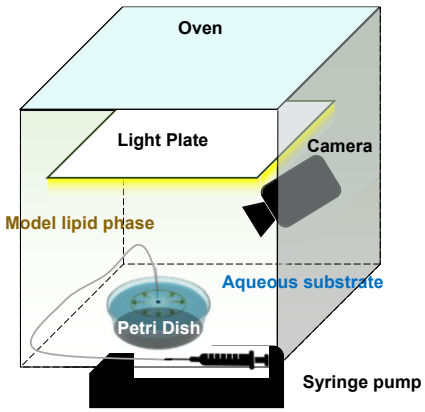

Figure 2 Representative diagram of the experimental setup developed to observe the spreading of the lipid droplet on the aqueous substrate.

2.3.2 Image processing

The spreading videos were transformed into a succession of images and analyzed using a plug-in machine learning tool called Trainable Weka Segmentation, available in ImageJ, to extract the evolution of spreading radius over time. We trained this tool to recognize different areas on an image to discern what belongs to the lipid droplet and what belongs to the aqueous substrate (Figure 3b) and apply it to the stack of images. For each tested formula, each

experiment was repeated atleast 5 times to ensure consistency and for each of them, 30 to 45 frames were analyzed with the help of ImageJ. The plug-in return a lipid droplet probability map where the pixels in white belonged to the lipid droplet and the ones in black were simply background (Figure 3c). From this map, it was possible to apply a threshold (between 0 and 255) and to use ImageJ Analyse Particle command to easily locate the lipid droplet (Figure 3d) on each frame. Analyse Particle command returned the area of the lipid droplet. All droplets were assumed to be perfectly circular and the calculated radius was plotted as a function of time. The data was fitted using power law function: ($r(t) = k.t^n$). Once all the replicas have been analyzed, the final distribution was obtained by averaging the parameters, k and n.

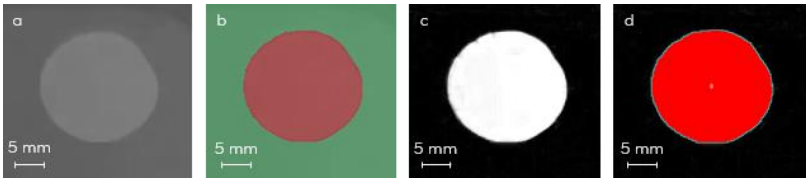

Figure 3 Steps of the image processing carried out : a). original black and white frame; b). separation of the image into two classes by the Trainable Weka Segmentation plugin; c). probability map of lipid drop; and d). drop detected by ImageJ.

3. Results

3.1 *Clinical results*

Based on the ocular subscores, shampoos were classified as good and poor clinical profile. Out of the 26 shampoos studies, 12 were very well tolerated while the rest 14 had poor clinical profile (Table II).

Table II Repartition of the shampoos used in the study as good and poor ocular profile.

	Good clinical profile	***Poor clinical profile***
Shampoos	12	14

3.2 Spreading dynamics

3.2.1 Qualitative approach – Droplet Profile

We observed the stability of the lipid phase droplets during spreading process. It was seen that for some formulas, the droplet spread uniformly and eventually breaking over time (Figure 4a). This breaking of the droplet sometimes appeared in the form of digitations or serations (Figure 4b) while other times, it appeared as holes which was reminiscent of the dewetting phenomenon (Figure 4c). In other cases, the droplet remained stable on the aqueous substrate (Figure 4d). Based on these observations, droplet profiles were categorized as deformed (exhibiting digitations at the contact line), dewetted (showing hole formation) or stable.

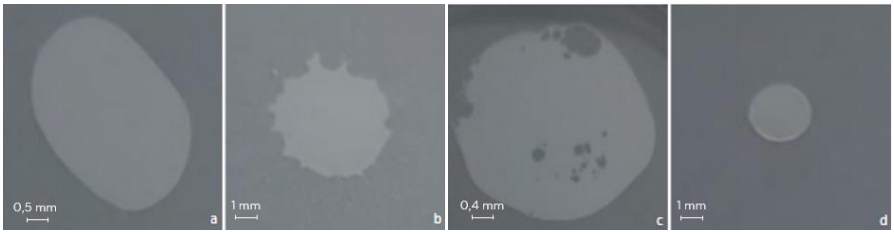

Figure 4 Different profiles of evolution of a lipid phase dropley on the aqueous substrate, a). uniform spreading, b). digitations along the contact line, c). dewetting, d). stable droplet.

To better analyse the behaviour of the unstable lipid droplets, we defined 3 parameters : (1). Breakup time (BUT), which corresponds to the time between the deposition of the lipid drop and the appearance of instabilities like holes and digitations, (2). Percentage coverage, which is the proportion of the area occupied by the lipid droplet at BUT in reference to the area of the substrate (or when it ceases to spread as in the case of a stable droplet), and (3). Spreading exponent (n), which is evaluated by fitting the evolution of the radius of the spreading droplet with time to Tanner's law and it indicates how fast the droplet spreads. By cross-linking the results of the different droplet profiles (as shown in Figure 4) with the clinical results, the behavior of the lipid droplet (deformation along the contact line, dewetting and stability) can be predicted according to the rate of spreading (n) and the percentage of coverage of the droplet at BUT or at steady state for stable drops. In this way, it can be assumed that the mechanisms leading to breaking or the deformation of the lipid drop are quite different (Figure 5).

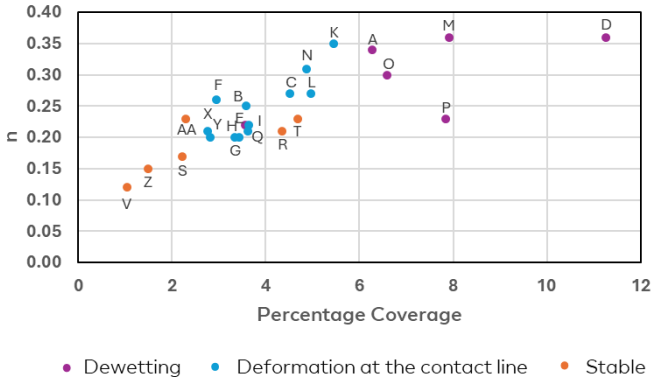

Figure 5 Graph representing the parameter n of the spreading law as a function of the percentage of coverage of the lipid droplet.

Furthermore, when comparing the droplet's behavior on the aqueous substrate with the clinical profiles, it was observed that 6 out of the 7 shampoos in the stable-droplet category exhibited poor clinical results.

Table III Distribution of clinical profiles for each droplet profile.

Gout Progression Profile	Good clinical profile	Poor clinical profile
Stable	1	6
Deformation	8	5
Dewetting	3	3

3.2.2 Quantitave approach – Droplet Spreading

We investigated the spreading and the appearance of instabilities of the model lipid phase on aqueous substrate (1:1 of model aqueous phase + 1% shampoo diluted in milliQ). Evidently, spreading of lipid droplet exhibited different behaviour with different shampoos. Figure 6 below shows the evolution of the lipid droplet over aqueous substrate under white light.

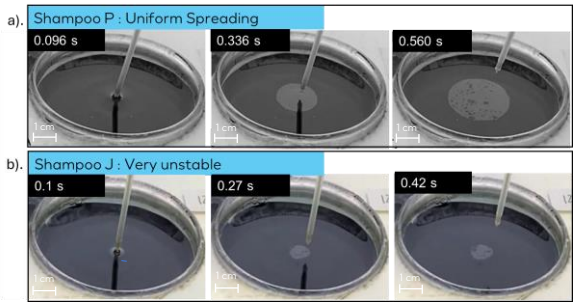

Figure 6 Shows the snapshots of the spreading of the lipid phase on aqueous phase mixed with 1% diluted a). Shampoo P, and b). Shampoo J.

In Shampoo P, we see the appearance of holes and instabilities at 0.56 s, however, the droplet spread quite uniformly initially. It was seen that the film eventually disappeared likely due to the dissolution attributed to the presence of surfactants in the shampoo. In the other case such as Shampoo J in Figure 6b, the droplet did not spread indicating a negative spreading coefficient. The evolution of the lipid droplet radius as a function of time was plotted (Figure 7a). Clearly, the spreading of the lipid layer obeys Tanner's law. Using power law regression, we determined the spreading parameters, n and k (with R^2 always more than 0.9). We then plotted the parameters, n and k of lipid spreading for different shampoos in relation to their ocular tolerance potential (Figure 7b & c). As can be seen, no direct correlation is observed between the spreading parameters, n and k and the ocular profile, which is in line with our hypothesis that the discomfort happens due to the disruption of the tear film.

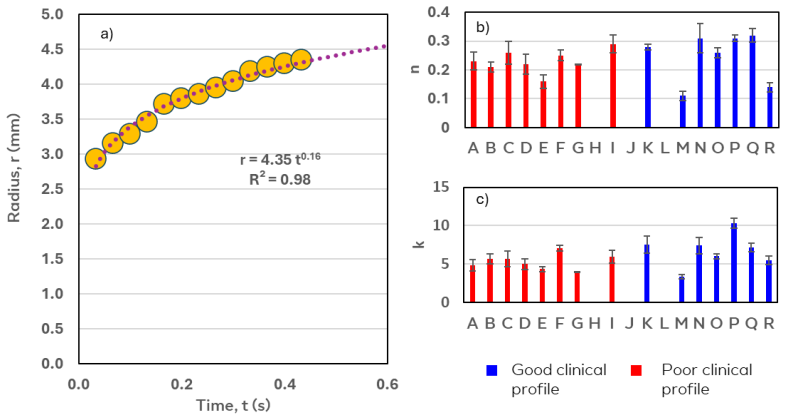

Figure 7 (a). Plot of the radius of the lipid droplet as a function of time, (b) and (c). histogram of spreading parameters $n\ and\ k$ evaluated for different shampoos in relation with the ocular profile.

In order to take into account all the factors possibly impacting the disruption of the lipid layer, we mapped the parameter, n, which is indicative of how fast the lipid layer spreads with the

BUT (which is the time at which the film breaks) for all shampoos with good and poor ocular profile in Figure 8.

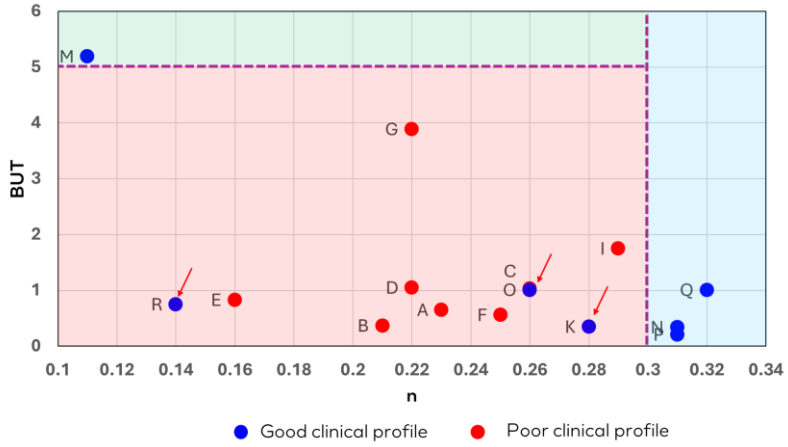

Figure 8 Graph representing the BUT as a function of the parameter n of the spreading law for all shampoos (green zone: good ocular tolerance formula; red zone: poor ocular tolerance formula; blue zone: no conclusion).

Here, we observe clustering of shampoos having different clinical profiles (in blue and red are shampoos with good and poor clinical profile respectively in Figure 8, separated by thresholds (purple dotted line) on n and BUT.

- Threshold on BUT → 5 s (Horizontal)
- Threshold on n → 0.3 (Vertical)

Bringing our focus to the vertical threshold, that is n = 0.3, we observe 2 cases :

Case 1: n < 0.3

This is typically the case where the droplet spreads slowly. From our experiments, it was seen that the instabilities usually arise at the contact line and eventually leading to the "breaking" of the droplet. The question of how quickly the instabilities arise can explain the discomfort potential of the shampoo. In this case, the aforementioned threshold on BUT (= 5 s) plays an important role. When BUT < 5 s, it means that even though the droplet is spreading very slowly, it breaks early in the spreading process (represented by the red zone in Figure 8). We found that the shampoos in this zone were more likely to have poor clinical profile, however, 3 false positives for shampoo R, C & K also were observed in this zone. Interestingly, when the BUT exceeds the threshold (i.e BUT > 5 s) for these slowly spreading droplets (zone green in Figure 8), the shampoo was found be very well tolerated.

Case 2: n > 0.3

This is the case where the lipid droplet spreads faster and over a large area (zone blue in Figure 8). We assume the dominance of dewetting phenomenon that is negative spreading coefficient (S < 0) in this zone. All 3 shampoos in this zone had good clinical profile.

$$Spreading\ parameter, S = \gamma_{ag} - \gamma_{al} - \gamma_{lg}$$

where, γ_{ag} is the aqueous substrate-gas surface tension, γ_{al} is the aqueous substrate-lipid surface tension and γ_{lg} is the lipid-gas surface tension.

4. Discussion

The results of this study suggest the potential for developing a predictive method for eye tolerance of formulations based solely on physicochemical properties. As hypothesized, distinct droplet spreading behaviors were observed for different shampoos. Droplet profiles ranged from stable droplets to highly deformed droplets with digitations and holes. While shampoos associated with distorted droplet spreading exhibited varied clinical profiles, those that showed stable droplets tended to be poor clinical profile. This observation supports the hypothesis that ocular discomfort may arise from the destabilization of the tear film's lipid layer. The observation of stable, non-spreading lipid droplets indicates a negative spreading coefficient for the system. However, in vivo, even with a negative spreading coefficient, the eyelid's action during blinking forces the lipid layer to spread into a thin film. Due to the negative spreading coefficient ($\boldsymbol{S}$ < 0), this thin film is inherently unstable and spontaneously reorganizes via dewetting phenomena. Consequently, holes appear and expand within the lipid layer, compromising its ability to protect the aqueous layer from evaporation. From the mapping of n with BUT, we find different clustering of shampoos with good and poor clinical results, separated by a threshold of n = 0.3 and BUT = 5 s. When n < 0.3, we observed the well tolerated shampoo above BUT threshold (green zone in Figure 8) and poorly tolerated shampoos below 5 s (red zone in Figure 8) with an exception of 3 shampoos that are considered false positives. This 5 s threshold aligns with the typical blink interval in healthy individuals, during which the lipid layer is replenished. When the lipid layer breaks down before this natural replenishment (BUT < 5 s), the resulting disruption can lead to discomfort. Conversely, when the breakup time equals or exceeds the blink interval, the eye may not perceive discomfort as the disrupted layer is rapidly replaced. However, unlike the stable droplet results, which were predominantly associated with dewetting and poor clinical profile, shampoos exhibiting n > 0.3, that is characterized by rapid spreading and presumed dewetting, were generally well-tolerated. While our hypothesis is that dewetting is linked to discomfort, the good tolerance observed for these shampoos with n > 0.3 needs further investigation. Furthermore, the impact of BUT in this regime (n > 0.3) remains unclear due to limited dataset across the BUT range, necessitating additional research to draw definitive conclusions. However, this methodology should be followed initially for a larger number of formulas for which clinical data are available. In this way, it will be possible to further refine the thresholds chosen to separate the formulas of good and poor clinical profile.

5. Conclusion

This in vitro method demonstrates robust reproducibility and generates predictions of ocular discomfort that are largely consistent with clinical observations. These findings indicate that our novel physicochemical approach offers a promising in vitro method for predicting shampoo discomfort potential. This approach holds potential for broader application in assessing the discomfort potential of other cosmetic formulations and could significantly enhance preclinical ocular evaluation strategies, optimizing clinical trials, reducing costs, and minimizing the number of formulations for clinical testing.

References

1. Debbasch C, Ebenhahn C, Dami N, Pericoi M, Van den Berghe C, Cottin M, Nohynek GJ. Eye irritation of low-irritant cosmetic formulations: correlation of in vitro results with clinical data and product composition. Food Chem Toxicol. 2005;43(1):155-65.
2. Nichols KK, Begley CG, Caffery B, Jones LA. Symptoms of ocular irritation in patients diagnosed with dry eye. Optom Vis Sci. 1999 Dec;76(12):838-44.
3. Zhang J, Begley CG, Situ P, Simpson T, Liu H. A link between tear breakup and symptoms of ocular irritation. Ocul Surf. 2017;15(4):696-703.
4. Pflugfelder SC, Tseng SC, Sanabria O, Kell H, Garcia C, Felix C, Feuer W, Reis BL. Evaluation of subjective assessments and objective diagnostic tests for diagnosing tear-film disorders known to cause ocular irritation. Cornea. 1998 Jan;17(1):38.
5. Craig JP, Tomlinson A. Importance of the lipid layer in human tear film stability and evaporation. Optom Vis Sci. 1997 Jan;74(1):8-13.
6. Dilly PN. Structure and function of the tear film. In: Lacrimal gland, tear film, and dry eye syndromes: basic science and clinical relevance. 1994. p. 239-47.
7. Blackie CA, Solomon JD, Scaffidi RC, Greiner JV, Lemp MA, Korb DR. The relationship between dry eye symptoms and lipid layer thickness. Cornea. 2009 Jul;28(7):789-94.
8. The definition and classification of dry eye disease: report of the Definition and Classification Subcommittee of the International Dry Eye Workshop (2007). Ocul Surf. 2007;5:75-92.
9. Tsubota K, Hata S, Okusawa Y, Egami F, Ohtsuki T, Nakamori K. Quantitative videographic analysis of blinking in normal subjects and patients with dry eye. Arch Ophthalmol. 1996 Jun;114(6):715-20.
10. Herok GH, Mudgil P, Millar TJ. The effect of meibomian lipids and tear proteins on evaporation rate under controlled in vitro conditions. Curr Eye Res. 2009;34:589-97.
11. King-Smith PE, Fink BA, Hill RM, Koelling KW, Tiffany JM. The thickness of the tear film. Curr Eye Res. 2004;29:357-68.
12. The epidemiology of dry eye disease: report of the Epidemiology Subcommittee of the International Dry Eye WorkShop (2007). Ocul Surf. 2007;5:93-107.
13. Bursztyn I. Evaporation reduction of water. Nature. 1966;211:521.
14. Bron AJ, Tiffany JM, Gouveia SM, Yokoi N, Voon LW. Functional aspects of the tear film lipid layer. Exp Eye Res. 2004;78:347-60.
15. Tanner LH. The spreading of silicone oil drops on horizontal surfaces. J Phys D Appl Phys. 1979;12(9):1473.
16. Mansfield WW. Effect of surface films on the evaporation of water. Nature. 1953;172:1101.
17. Rondot B, Handjani-Vila RM. A new in vitro method for ocular irritancy caused by surfactants. In: 14th IFSCC congress; 1986.
18. Butovich IA. Tear film lipids. Exp Eye Res. 2013;117:4-27.